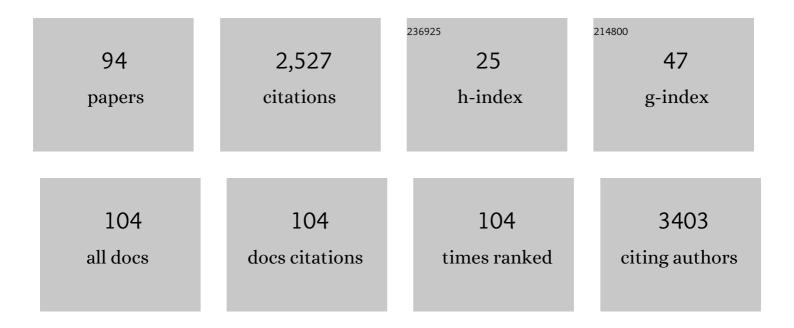
List of Publications by Year in descending order

Source: https://exaly.com/author-pdf/2323755/publications.pdf Version: 2024-02-01



#	Article	IF	CITATIONS
1	Lymph node targeting strategies to improve vaccination efficacy. Journal of Controlled Release, 2017, 267, 47-56.	9.9	207
2	Targeted delivery of low-dose dexamethasone using PCL–PEG micelles for effective treatment of rheumatoid arthritis. Journal of Controlled Release, 2016, 230, 64-72.	9.9	171
3	Targeting NF-kB signaling with polymeric hybrid micelles that co-deliver siRNA and dexamethasone for arthritis therapy. Biomaterials, 2017, 122, 10-22.	11.4	161
4	Combining photothermal therapy and immunotherapy against melanoma by polydopamine-coated Al ₂ O ₃ nanoparticles. Theranostics, 2018, 8, 2229-2241.	10.0	116
5	pH-sensitive polymeric micelles for targeted delivery to inflamed joints. Journal of Controlled Release, 2017, 246, 133-141.	9.9	114
6	Highly Enantioselective Synthesis of γ-Hydroxy-α,β-acetylenic Esters by Asymmetric Alkyne Addition to Aldehydes. Angewandte Chemie - International Edition, 2006, 45, 122-125.	13.8	111
7	Recent advances in nanomedicines for the treatment of rheumatoid arthritis. Biomaterials Science, 2017, 5, 1407-1420.	5.4	100
8	Reinforced conducting hydrogels prepared from the in situ polymerization of aniline in an aqueous solution of sodium alginate. Journal of Materials Chemistry A, 2014, 2, 16516-16522.	10.3	93
9	Enantioselective Fluorescent Recognition of Amino Alcohols by a Chiral Tetrahydroxyl 1,1â€~-Binaphthyl Compound. Journal of Organic Chemistry, 2007, 72, 97-101.	3.2	82
10	Monometallic complexes of 1,4,7,10-tetraazacyclododecane containing an imidazolium side: Synthesis, characterization, and their interaction with plasmid DNA. Bioorganic and Medicinal Chemistry, 2006, 14, 4151-4157.	3.0	79
11	Highly Reactive Porphyrinâ^'Ironâ^'Oxo Derivatives Produced by Photolyses of Metastable Porphyrinâ^'Iron(IV) Diperchlorates. Journal of the American Chemical Society, 2009, 131, 2621-2628.	13.7	71
12	Quantitative Production of Compound I from a Cytochrome P450 Enzyme at Low Temperatures. Kinetics, Activation Parameters, and Kinetic Isotope Effects for Oxidation of Benzyl Alcohol. Journal of the American Chemical Society, 2009, 131, 10629-10636.	13.7	58
13	Fluoride induces apoptosis via inhibiting SIRT1 activity to activate mitochondrial p53 pathway in human neuroblastoma SH-SY5Y cells. Toxicology and Applied Pharmacology, 2018, 347, 60-69.	2.8	58
14	Electrochemical immunosensor for detecting the spore wall protein of Nosema bombycis based on the amplification of hemin/G-quadruplex DNAzyme concatamers functionalized Pt@Pd nanowires. Biosensors and Bioelectronics, 2014, 60, 118-123.	10.1	47
15	A crystalline covalent organic framework embedded with a crystalline supramolecular organic framework for efficient iodine capture. Journal of Materials Chemistry A, 2021, 9, 16961-16966.	10.3	43
16	Sirtuin 6 inhibits myofibroblast differentiation via inactivating transforming growth factorâ€Î²1/Smad2 and nuclear factorâ€ÎºB signaling pathways in human fetal lung fibroblasts. Journal of Cellular Biochemistry, 2019, 120, 93-104.	2.6	41
17	Rationally Designed Selfâ€Assembling Nanoparticles to Overcome Mucus and Epithelium Transport Barriers for Oral Vaccines against <i>Helicobacter pylori</i> . Advanced Functional Materials, 2018, 28, 1802675.	14.9	37
18	Enzyme-assisted cycling amplification and DNA-templated in-situ deposition of silver nanoparticles for the sensitive electrochemical detection of Hg2+. Biosensors and Bioelectronics, 2016, 86, 630-635.	10.1	36

#	Article	IF	CITATIONS
19	Efficient entanglement concentration for concatenated Greenberger–Horne–Zeilinger state with the cross-Kerr nonlinearity. Quantum Information Processing, 2016, 15, 1669-1687.	2.2	31
20	Ghrelin Restores the Disruption of the Circadian Clock in Steatotic Liver. International Journal of Molecular Sciences, 2018, 19, 3134.	4.1	30
21	Combined delivery of a TGF-Î ² inhibitor and an adenoviral vector expressing interleukin-12 potentiates cancer immunotherapy. Acta Biomaterialia, 2017, 61, 114-123.	8.3	29
22	Bio-inspired polymer envelopes around adenoviral vectors to reduce immunogenicity and improve in vivo kinetics. Acta Biomaterialia, 2016, 30, 94-105.	8.3	28
23	Multi-Year Comparison of CO2 Concentration from NOAA Carbon Tracker Reanalysis Model with Data from GOSAT and OCO-2 over Asia. Remote Sensing, 2020, 12, 2498.	4.0	27
24	Transcriptome sequencing and differential gene expression analysis in Viola yedoensis Makino (Fam.) Tj ETQq0 0 Communications, 2015, 459, 60-65.	0 rgBT /Ov 2.1	verlock 10 Tf 26
25	Kinetics and Activation Parameters for Oxidations of Styrene by Compounds I from the Cytochrome P450 _{BM-3} (CYP102A1) Heme Domain and from CYP119. Biochemistry, 2009, 48, 9140-9146.	2.5	25
26	An amplified electrochemical proximity immunoassay for the total protein of Nosema bombycis based on the catalytic activity of Fe3O4NPs towards methylene blue. Biosensors and Bioelectronics, 2016, 81, 382-387.	10.1	25
27	Optimized in vivo performance of acid-liable micelles for the treatment of rheumatoid arthritis by one single injection. Nano Research, 2019, 12, 421-428.	10.4	24
28	Astragaloside IV inhibits hepatocellular carcinoma by continually suppressing the development of fibrosis and regulating pSmad3C/3L and Nrf2/HO-1 pathways. Journal of Ethnopharmacology, 2021, 279, 114350.	4.1	24
29	Diverse Transformations of Chiral Propargylic Alcohols Generated by BINOL-Catalyzed Alkyne Addition to Aldehydes. Synlett, 2013, 24, 1340-1363.	1.8	23
30	1,1′-Binaphthyl ligands with bulky 3,3′-tertiaryalkyl substituents for the asymmetric alkyne addition to aromatic aldehydes. Tetrahedron, 2007, 63, 4422-4428.	1.9	22
31	Validation of GOSAT and OCO-2 against In Situ Aircraft Measurements and Comparison with CarbonTracker and GEOS-Chem over Qinhuangdao, China. Remote Sensing, 2021, 13, 899.	4.0	22
32	Engineering P450 Peroxygenase to Catalyze Highly Enantioselective Epoxidation of <i>cis</i> â€Î²â€Methylstyrenes. Chemistry - A European Journal, 2016, 22, 10969-10975.	3.3	21
33	Ghrelin ameliorates nonalcoholic steatohepatitis induced by chronic lowâ€grade inflammation via blockade of Kupffer cellÂM1 polarization. Journal of Cellular Physiology, 2021, 236, 5121-5133.	4.1	20
34	Optimization and quality assessment of adventitious roots culture in Panax quinquefolium L Acta Physiologiae Plantarum, 2014, 36, 713-719.	2.1	19
35	Synergistic enhancement of cytotoxicity against cancer cells by incorporation of rectorite into the paclitaxel immobilized cellulose acetate nanofibers. International Journal of Biological Macromolecules, 2020, 152, 672-680.	7.5	19
36	Assessing the development and treatment of rheumatoid arthritis using multiparametric photoacoustic and ultrasound imaging. Journal of Biophotonics, 2019, 12, e201900127.	2.3	18

#	Article	IF	CITATIONS
37	Blood pressure and renal function decline. Journal of Hypertension, 2015, 33, 136-143.	0.5	17
38	Effects of Nisin, Cecropin, and Penthorum chinense Pursh on the Intestinal Microbiome of Common Carp (Cyprinus carpio). Frontiers in Nutrition, 2021, 8, 729437.	3.7	17
39	Enhanced Turnover for the P450 119 Peroxygenase atalyzed Asymmetric Epoxidation of Styrenes by Random Mutagenesis. Chemistry - A European Journal, 2018, 24, 2741-2749.	3.3	16
40	Liposome mediated-CYP1A1 gene silencing nanomedicine prepared using lipid film-coated proliposomes as a potential treatment strategy of lung cancer. International Journal of Pharmaceutics, 2019, 566, 185-193.	5.2	16
41	Mechanistic Study on a BINOL–Coumarin-Based Probe for Enantioselective Fluorescent Recognition of Amino Acids. Journal of Organic Chemistry, 2020, 85, 6352-6358.	3.2	16
42	Directed evolution of Streptomyces lividans xylanase B toward enhanced thermal and alkaline pH stability. World Journal of Microbiology and Biotechnology, 2009, 25, 93-100.	3.6	15
43	Highly enantioselective addition of linear alkyl alkynes to aromatic aldehydes. Tetrahedron: Asymmetry, 2011, 22, 1142-1146.	1.8	15
44	Enhanced turnover rate and enantioselectivity in the asymmetric epoxidation of styrene by new T213G mutants of CYP 119. RSC Advances, 2014, 4, 27526-27531.	3.6	15
45	Characterization of a thermostable phytase from Bacillus licheniformis WHU and further stabilization of the enzyme through disulfide bond engineering. Enzyme and Microbial Technology, 2020, 142, 109679.	3.2	15
46	Tissue factor pathway inhibitor-2 induced hepatocellular carcinoma cell differentiation. Saudi Journal of Biological Sciences, 2017, 24, 95-102.	3.8	14
47	Excitation of One Fluorescent Probe at Two Different Wavelengths to Determine the Concentration and Enantiomeric Composition of Amino Acids. Organic Letters, 2019, 21, 9036-9039.	4.6	14
48	Biogenic iron mineralization of polyferric sulfate by dissimilatory iron reducing bacteria: Effects of medium composition and electric field stimulation. Science of the Total Environment, 2019, 684, 466-475.	8.0	14
49	ALKBH5 promotes cadmium-induced transformation of human bronchial epithelial cells by regulating PTEN expression in an m6A-dependent manner. Ecotoxicology and Environmental Safety, 2021, 224, 112686.	6.0	13
50	Associations between Serum-Intact Parathyroid Hormone, Serum 25-Hydroxyvitamin D. Oral Vitamin D Analogs and Metabolic Syndrome in Peritoneal Dialysis Patients: A Multi-Center Cross-Sectional Study. Peritoneal Dialysis International, 2014, 34, 447-455.	2.3	12
51	Enhancement of keratin-degradation ability of the keratinase KerBL from Bacillus licheniformis WHU by proximity-triggered chemical crosslinking. International Journal of Biological Macromolecules, 2020, 163, 1458-1470.	7.5	12
52	PLA ₂ -Triggered Release of Drugs from Self-Assembled Lipid Tubules for Arthritis Treatments. ACS Applied Bio Materials, 2020, 3, 6488-6496.	4.6	12
53	Structure of a Dimeric BINOL-Imine-Zn(II) Complex and Its Role in Enantioselective Fluorescent Recognition. Inorganic Chemistry, 2020, 59, 17992-17998.	4.0	11
54	Comparative analysis of the gut microbiota of grass carp fed with chicken faeces. Environmental Science and Pollution Research, 2020, 27, 32888-32898.	5.3	11

#	Article	IF	CITATIONS
55	Synthesis of small cyclic peptides containing disulfide bonds. Arkivoc, 2006, 2006, 148-154.	0.5	11
56	<i>O</i> â€Alkylation of 3â€Formylâ€BINOL and Its Strong Effect on the Fluorescence Recognition of 1,3â€Diaminopropane. European Journal of Organic Chemistry, 2018, 2018, 4972-4977.	2.4	9
57	Preparation of pyrido[1,2-c][1,2,4]triazole-based π-conjugated triazene as a Fe3+ ion fluorescent sensor. Chinese Chemical Letters, 2019, 30, 1059-1062.	9.0	9
58	Insight Into the Effects of Nisin and Cecropin on the Oral Microbial Community of Rats by High-Throughput Sequencing. Frontiers in Microbiology, 2020, 11, 1082.	3.5	9
59	Nocturnal Systolic Hypertension and Adverse Prognosis in Patients with CKD. Clinical Journal of the American Society of Nephrology: CJASN, 2021, 16, 356-364.	4.5	9
60	Enhancement of Activity and Thermostability of Keratinase From Pseudomonas aeruginosa CCTCC AB2013184 by Directed Evolution With Noncanonical Amino Acids. Frontiers in Bioengineering and Biotechnology, 2021, 9, 770907.	4.1	9
61	Spatiotemporal Investigation of Near-Surface CO ₂ and Its Affecting Factors Over Asia. IEEE Transactions on Geoscience and Remote Sensing, 2022, 60, 1-16.	6.3	9
62	Total Synthesis of Chiral Falcarindiol Analogues Using BINOL-Promoted Alkyne Addition to Aldehydes. Molecules, 2016, 21, 112.	3.8	7
63	Dynamic Mapping and Quality of Service Driven Re-Embedding in Virtualization Environment. , 2019, , .		7
64	White-coat hypertension and incident end-stage renal disease in patients with non-dialysis chronic kidney disease: results from the C-STRIDE Study. Journal of Translational Medicine, 2020, 18, 238.	4.4	7
65	Astragaloside IV suppresses migration and invasion of TGF-β1-induced human hepatoma HuH-7 cells by regulating Nrf2/HO-1 and TGF-I²1/Smad3 pathways. Naunyn-Schmiedeberg's Archives of Pharmacology, 2022, 395, 397-405.	3.0	7
66	Highly enantioselective catalytic methyl propiolate addition to both aromatic and aliphatic aldehydes. Tetrahedron: Asymmetry, 2016, 27, 428-435.	1.8	6
67	Highly Enantioselective Synthesis and Anticancer Activities of Chiral Conjugated Diynols. ChemBioChem, 2018, 19, 2293-2299.	2.6	6
68	Enhanced Activity and Substrate Specificity by Siteâ€Đirected Mutagenesis for the P450 119 Peroxygenase Catalyzed Sulfoxidation of Thioanisole. ChemistryOpen, 2019, 8, 1076-1083.	1.9	6
69	Reinforcement of phenylalanine-based supramolecular hydrogels by hybridizing poly(N-isopropylacrylamide) nanogels. RSC Advances, 2014, 4, 22380-22386.	3.6	5
70	Access to Fluorescent Azines from Nâ€Heterocyclic Carbene Precursors and <i>N</i> â€Tosylhydrazones. Advanced Synthesis and Catalysis, 2017, 359, 1825-1830.	4.3	5
71	Comparative Analyses of the Transcriptome and Proteome of Escherichia coli C321.â–3A and Further Improving Its Noncanonical Amino Acids Containing Protein Expression Ability by Integration of T7 RNA Polymerase. Frontiers in Microbiology, 2021, 12, 744284.	3.5	5
72	Genome-wide identification and expression pattern analysis of novel chemosensory genes in the German cockroach Blattella germanica. Genomics, 2022, 114, 110310.	2.9	5

#	Article	IF	CITATIONS
73	Optimization of balloon-type bubble bioreactor angle and methyl jasmonate concentration to enhance metabolite production in adventitious roots of Pseudostellaria heterophylla. Research on Chemical Intermediates, 2015, 41, 5555-5563.	2.7	4
74	Utilization of antihypertensive drugs among chronic kidney disease patients: Results from the Chinese cohort study of chronic kidney disease (C‧TRIDE). Journal of Clinical Hypertension, 2020, 22, 57-64.	2.0	4
75	Highly Diastereoselective Synthesis of 2,2-Disubstituted Cyclopentane-1,3-diols via Stepwise Ketone Reduction Enabling Concise Chirality Construction. Journal of Organic Chemistry, 2020, 85, 9599-9606.	3.2	4
76	CircSPAG16 suppresses cadmiumâ€induced transformation of human bronchial epithelial cells by decoying PIP5K11± to inactivate Akt. Molecular Carcinogenesis, 2021, 60, 582-594.	2.7	4
77	Influence of step-wise aeration treatment on biomass and bioactive compounds of Panax ginseng adventitious root in balloon-type bubble bioreactor. Research on Chemical Intermediates, 2015, 41, 623-629.	2.7	3
78	A Prime–Boost Strategy Combining Intravaginal and Intramuscular Administration of Homologous Adenovirus to Enhance Immune Response Against HIV-1 in Mice. Human Gene Therapy, 2016, 27, 219-229.	2.7	3
79	Effects of temperature and pressure on the nucleation and growth of silver clusters from supersaturated vapor: A molecular dynamics analysis. International Journal of Modern Physics B, 2017, 31, 1750057.	2.0	3
80	Selective detection of Cys and GSH by using one fluorescent probe at two excitation wavelengths. Tetrahedron Letters, 2020, 61, 152462.	1.4	3
81	A novel circular RNA, circPUS7 promotes cadmium-induced transformation of human bronchial epithelial cells by regulating Kirsten rat sarcoma viral oncogene homolog expression via sponging miR-770. Metallomics, 2021, 13, .	2.4	3
82	Characterization of novel Tn7-derivatives and Tn7-like transposon found in Proteus mirabilis of food-producing animal origin in China. Journal of Global Antimicrobial Resistance, 2022, , .	2.2	3
83	Asymmetric synthesis of 2,6-substituted dihydropyrone catalyzed by 3-monosubstituted and 3,3′-bisubstituted BINOL titanium complexes. Chemical Papers, 2008, 62, .	2.2	2
84	Construction of functional chimeras of syntaxin-1A and its yeast orthologue, and their application to the yeast cell-based assay for botulinum neurotoxin serotype C. Biochimica Et Biophysica Acta - General Subjects, 2019, 1863, 129396.	2.4	2
85	Synthesis, Anticancer Activity, Structureâ€Activity Relationship and Mechanistic Investigations of Falcarindiol Analogues. ChemMedChem, 2021, 16, 3569-3575.	3.2	2
86	Copper-catalyzed cleavage of benzyl ethers with (diacetoxyiodo)- benzene and p-toluenesulfonamide. Arkivoc, 2008, 2008, 103-108.	0.5	2
87	Distinct skin morphological and transcriptomic profiles between wild and albino Oscar Astronotus ocellatus. Comparative Biochemistry and Physiology Part D: Genomics and Proteomics, 2022, 41, 100944.	1.0	2
88	A Racemic Naphthyl oumarinâ€Based Probe for Quantitative Enantiomeric Excess Analysis of Amino Acids and Enantioselective Sensing of Amines and Amino Alcohols. ChemistryOpen, 2022, 11, .	1.9	2
89	Smad3 gene C-terminal phosphorylation site mutation exacerbates CCl4-induced hepatic fibrogenesis by promoting pSmad2L/C-mediated signaling transduction. Naunyn-Schmiedeberg's Archives of Pharmacology, 2021, 394, 1779-1786.	3.0	1
90	Synthesis and Biological Evaluation of Falcarinol-Type Analogues as Potential Calcium Channel Blockers. Journal of Natural Products, 2021, 84, 2138-2148.	3.0	1

#	Article	IF	CITATIONS
91	UNIFORM EMBEDDINGS OF FREE PRODUCTS INTO UNIFORMLY CONVEX BANACH SPACES. Bulletin of the London Mathematical Society, 2006, 38, 139-142.	0.8	Ο
92	Use of partial least-squares discriminant analysis to study the effects of gradual scale-up of culture, and optimization of bioreactor angle and aeration volume on culture of Panax quinquefolium L. adventitious roots in a 5-L balloon-type bubble bioreactor. Research on Chemical Intermediates, 2015, 41, 6707-6720.	2.7	0
93	HPLC Determination of Enantiomeric Purity for 1-Styrene-3-Hexyl Propynol. Journal of Chromatographic Science, 2016, 54, 1794-1799.	1.4	0
94	Synthesis and copolymerization of pentachlorophenyl acrylate monomers. Arkivoc, 2007, 2006, 75-82.	0.5	0